

# SEY studies in CSNS

Shenghua Liu,<sup>1,2,3,4</sup> Yudong Liu,<sup>1, 3,4,a)</sup> Pengcheng Wang,<sup>1,3,4</sup> Weibin Liu<sup>1,3,4</sup>, Guoxi Pei<sup>1</sup>, Lei Zeng,<sup>1,3</sup> Xiaoyang Sun,<sup>1,2,3</sup>

<sup>1</sup>Institute of High Energy Physics (IHEP), Chinese Academy of Sciences (CAS), Beijing 100049, China,

<sup>2</sup>University of Chinese Academy of Sciences (UCAS), Beijing 100049, China

<sup>3</sup>Dongguan Institute of Neutron Science (DINS), Dongguan 523803, China

<sup>4</sup>Key Laboratory of Particle Acceleration Physics and Technology, Institute of High Energy Physics (IHEP), Chinese Academy of Sciences (CAS), Beijing 100049, China

Mail:liushenghua@ihep.ac.cn

2018.5.3



# Outline

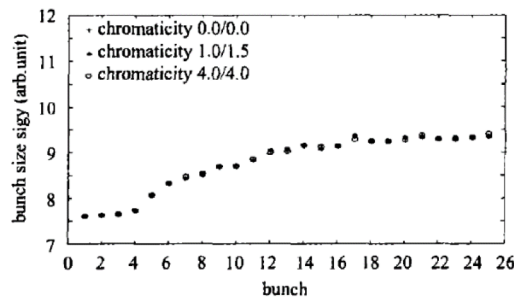
- Background and significance
- Measurement scheme
  - SEY and its dependence on incidence angle
  - Spatial distribution of secondary emission electrons
  - Spectrum distribution of secondary emission electrons
  - SEY depression as electron dose deposition
- Design and construct of SEE characteristics platform
- Experimental measurement and theoretical research
- Formula calculation and software simulation
- Summary and prospect

# Background and significance

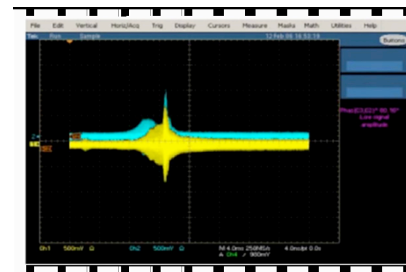
## Electron cloud effect and SEE characteristics of material

### Impact of electron cloud effect

(1) During the operation of the accelerator, the electron cloud effect in the vacuum pipe can cause **beam instability**, resulting in a decrease in **beam lifetime**, generation of **the detector background** and so on.



Simulated vertical bunch size blowup along the train



BPM traces of beam instability in the SNS accumulator ring

(2) The secondary electron multipacting effect occurring in the **high-frequency cavity** will cause frequent ignition of the high-frequency cavity, which severely limits the electromagnetic field intensity in the high-frequency cavity and even cause the failure of the high-frequency cavity system.

(3) Secondary electron emission **power deposition** in a beam screen in a superconducting low temperature environment may even result in quench protection of the entire superconductor system.

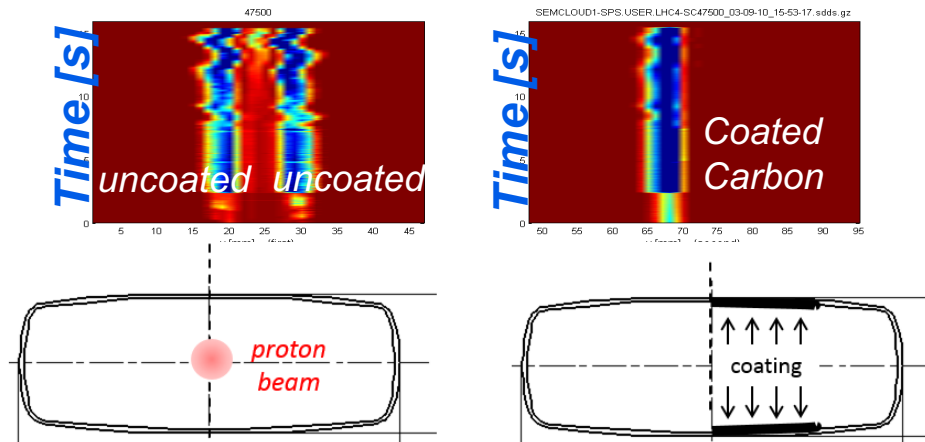
# Background and significance

## Source of electron cloud effect

- (1) Electrons generated by beam loss;
- (2) Electrons generated by ionization of residual gases in a vacuum chamber;
- (3) Secondary electrons;
- (4) For a proton accelerator such as CSNS, the stripping foil in the injection zone also generates a large amount of electrons;

## Secondary electron emission (SEE) characteristics of material

The core of electron cloud effect research is to study the establishment process of electron cloud. The generation of secondary electrons plays a decisive role in the process of establishing the electron cloud and the final density. Therefore, this subject studies the secondary electron emission characteristics of the material.



Electron cloud current in the SPS with an electron cloud detector

# Background and significance

## Vacuum chamber material commonly used in accelerators

Stainless steel

Aluminum

Copper

TiZrV and TiZrHfV

Ceramic coated TiN(**RCS ring of proton accelerator**): Ceramic can suppress the **eddy current effect** produced by the rapidly changing magnetic field in the magnets of the RCS ring, but the secondary electron emission coefficient of the ceramic is relatively high, so the TiN film is to be plated on the inner wall of the ceramic vacuum chamber.

# Background and significance

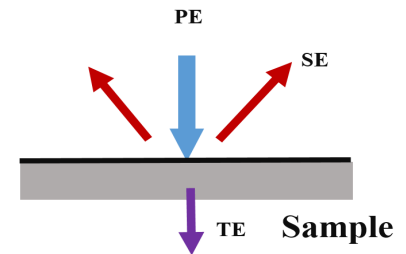
## Significance

- Reference for **selecting the best vacuum chamber material**
- Providing measurement data to **improve accelerator coating process**
- Providing data for **simulation of electron cloud**

# Measurement scheme

## Secondary electron Yield

$$\delta = n_{SE} / n_{PE}$$



## Complete secondary electron emission characteristics

SEY and its dependence on incidence angle

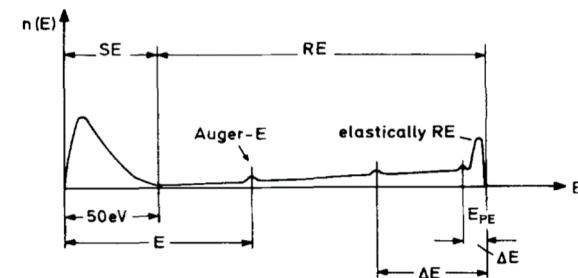
Spatial distribution of secondary emission electrons

Spectrum distribution of secondary emission electrons

SEY depression as electron dose deposition

$$REY = EREY + IREY$$

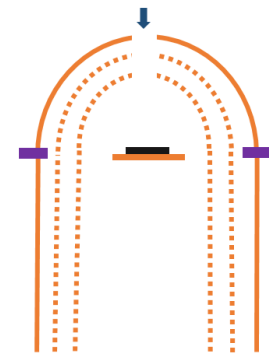
$$TSEY = SEY + REY$$



## Core: detector and sample holder

The detector is a three-layer structure: the outermost cap detector and wall detector are connected by an insulating ring, and the middle layer and the innermost layer are grid structures.

Sample holder: can be moved up and down in the vertical direction, and can be rotated in the axial direction from 0 to 180 degrees

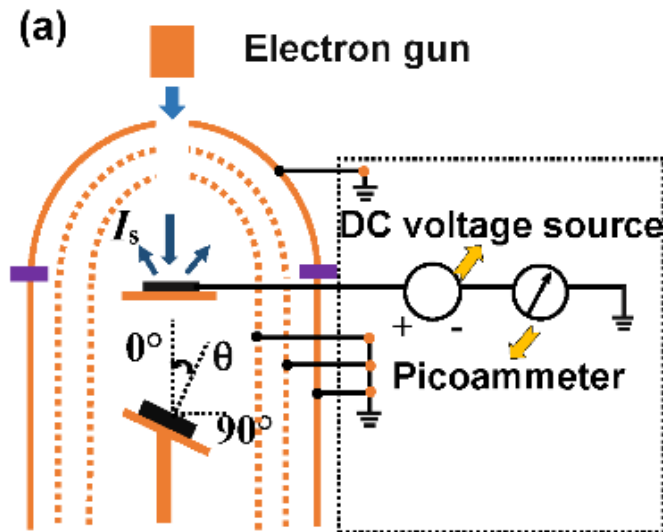


# Measurement scheme: SEY and its dependence on incidence angle

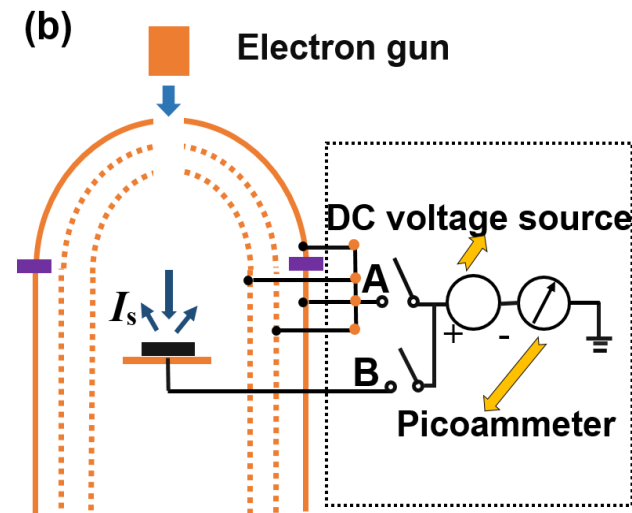
## ➤ Conductive sample

**Sample method :** -20V bias on sample  $\rightarrow I_t$  and +100V bias on sample  $\rightarrow I_p$ ,  $\delta = 1 - I_t/I_p$

**Collector method:** +50V bias on collector  $\rightarrow I_s$ , +50V bias on collector and sample  $\rightarrow I_p$ ,  
 $\delta = I_s/I_p$



Sample method

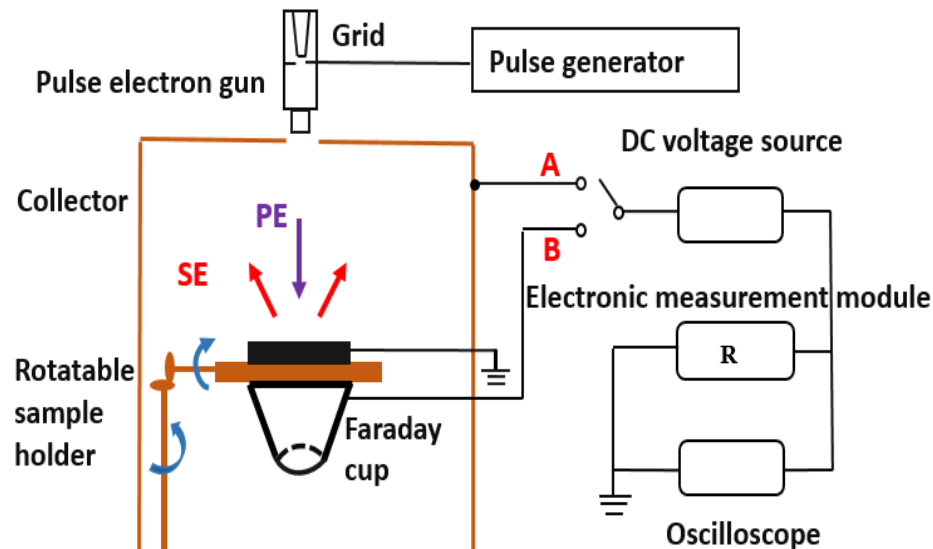


Collector method

# Measurement scheme: SEY and its dependence on incidence angle

## ➤ Insulating sample

- (1) Impulsator :  $150\text{ }\mu\text{s}$ ,  $f=25\text{ Hz}$  TTL signal ;
- (2) Faraday cup up, add  $+45\text{ V}$  bias on Faraday cup, **single pulse mode**, the pulse width is  $150\text{ }\mu\text{s}$ , incident electron current is  $I_p$ ;
- (3) Sample up, add  $+45\text{ V}$  bias on the complete detector, **single pulse mode**, secondary electron current  $I_s$ ;
- (4) Before the next measurement, neutralize the charge accumulated on the sample surface: add  $-45\text{ V}$  bias on the collector, **periodic pulse mode**, pulse duration  $1\sim 5\text{ s}$ , so that the secondary electron can return to the sample surface .

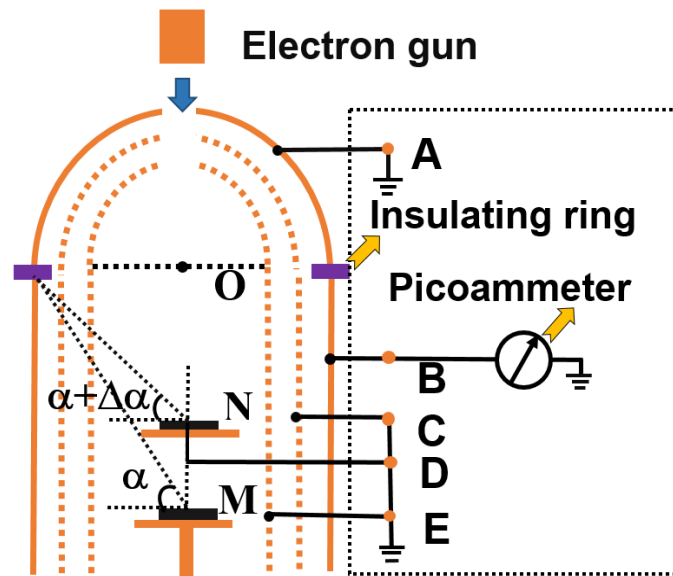


Neutralization method with negative bias on collector

# Measurement scheme: Spatial distribution of secondary emission electrons

**Core:** move the sample to different vertical positions to measure the current change on the cylinder type sidewall detector.

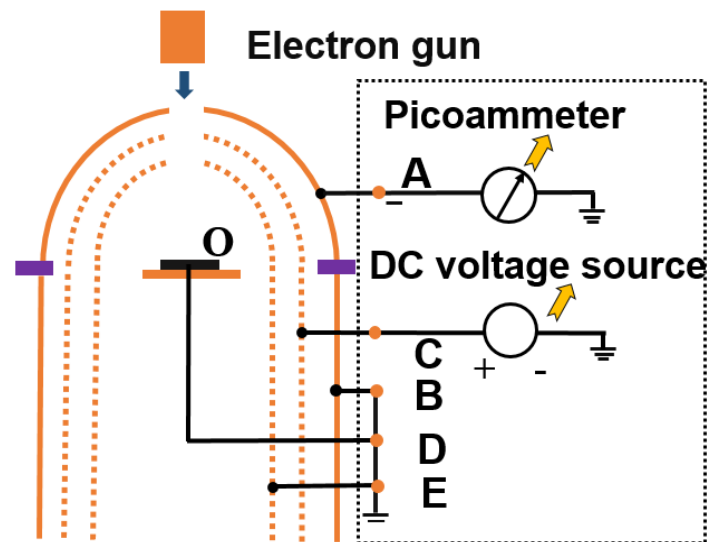
**Method:**  $M \rightarrow \alpha, I_\alpha$ ;  $N \rightarrow I_{\alpha+\Delta\alpha}$ ,  $\Delta\alpha$  and  $\Delta I_\alpha = I_\alpha - I_{\alpha+\Delta\alpha}$ ,  $20^\circ \sim 60^\circ$ ,  $1^\circ$ .



Difference method

# Measurement scheme: Spectrum distribution of secondary emission electrons

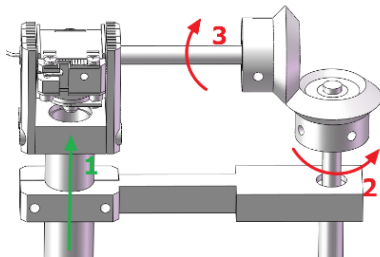
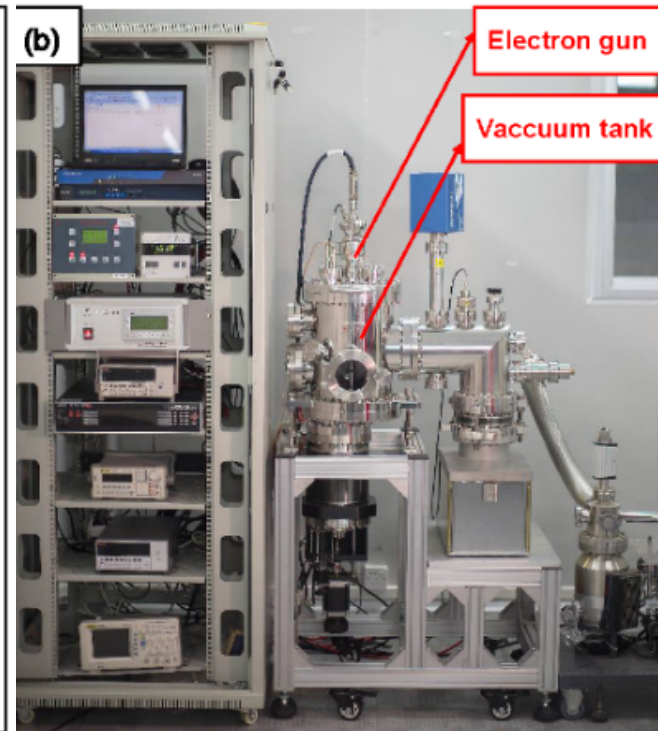
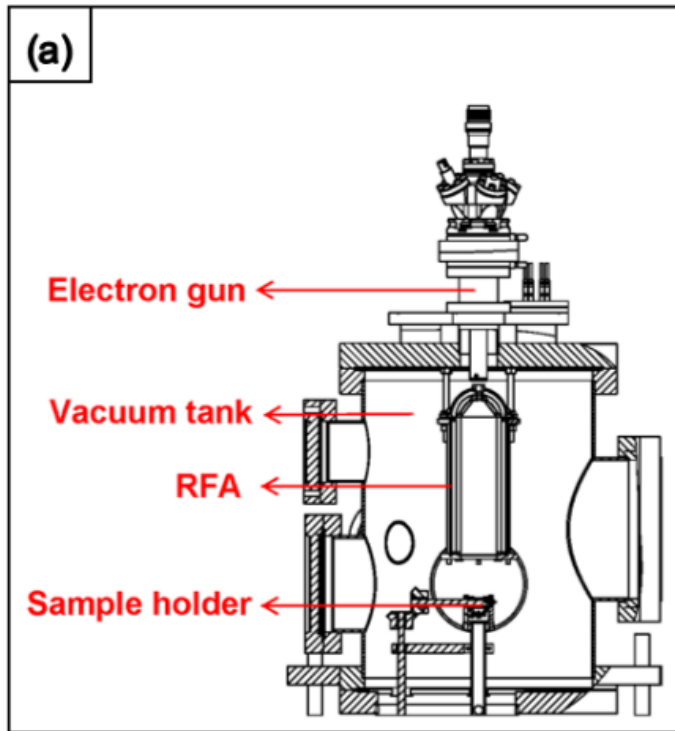
The sample table is placed at the center of the hemispherical detector. By changing the grid voltage  $U$ , the secondary electrons with energy less than  $eU$  are prevented, draw  $E(eU) - \Delta I_s$  curve as spectrum distribution.



Retarding field method

# Design and construct of SEE characteristics platform

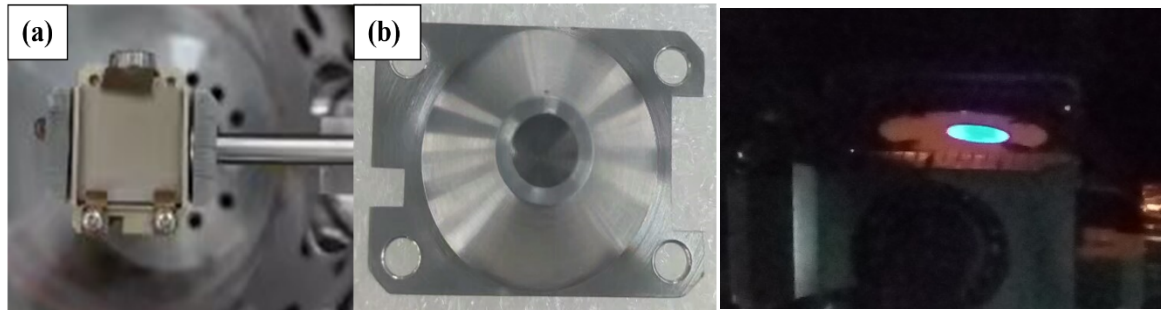
Measuring platform: vacuum system, measuring circuit system, data acquisition and equipment control system



# Design and construct of SEE characteristics platform

## Device advantage

- On the back of the rotatable sample holder, faraday cup(insulation sample measurement) and fluorescent target (focusing adjustment) can be installed according to the experimental requirements.

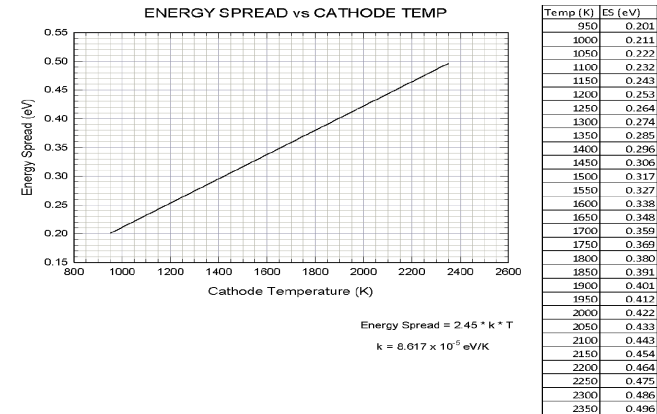


- Can measure the entire spatial distribution of secondary electrons
- Can measure the entire energy spectrum distribution of secondary electrons

# Experimental measurement and theoretical research

## Kimball Physics EFG-7-6644 electron gun

Beam Energy	100 eV-5000 eV
Beam Current	1 nA-100 $\mu$ A
Energy Spread	Approx 0.5 eV cathode thermal spread, calculated
Spot Size	1 mm-100 mm



(1) **Energy stability** :  $\pm 0.01\%$  per hour  $\pm 0.02\%$  per 8 hours at full output ;  
The dispersion of energy varying with filament temperature is as shown;  
Energy dispersion refers to the range of fluctuations centered around the set energy.

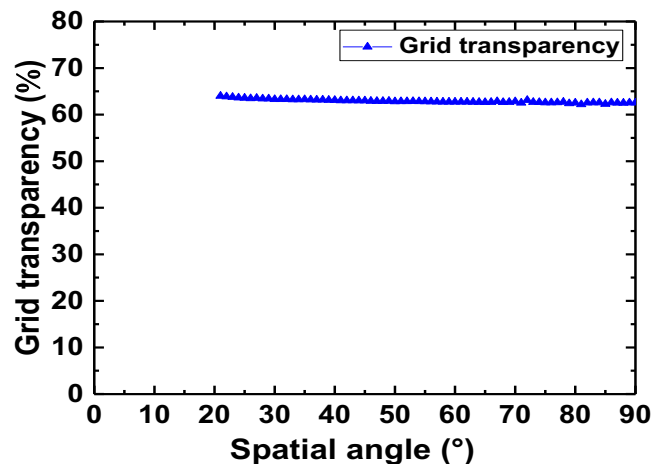
(2) **beam stability** : After warm up,  $\pm 0.1\%$  per hour with Emission Current Control (ECC) or  $\pm 10\%$  per hour without ECC

# Experimental measurement and theoretical research

## Grid transparency :

manufacturer :76%(vertical),  
experimental measurement: 63%

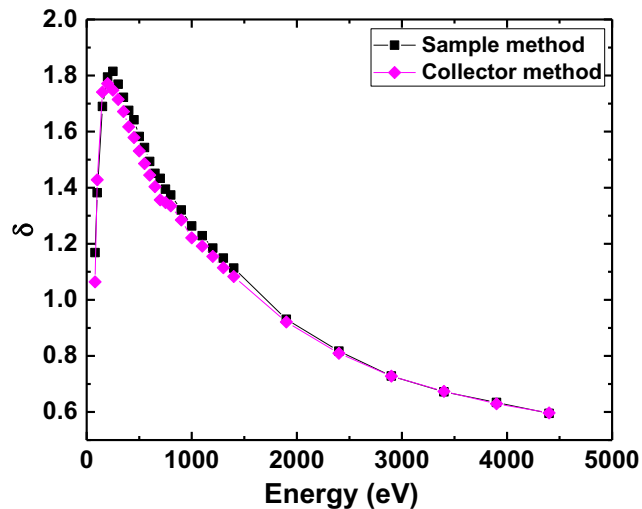
Secondary electron spatial distribution is measured by secondary electron current's **relative variation** under different spatial angle, and the range of almost constant grid transparency does not affect the measurement result.



# Experimental measurement and theoretical research: Comparison of sample method and collector method

**Conclusion:** The measurement results of the two methods are close , consistent with reference ( Valizadeh, Reza, et al.2014)

The sample method is easy to realize automatic measurement and control.



Cu	Epm (eV)	$\delta m$
sample method	300	1.80
collector method	300	1.70
Valizadeh, Reza, et al.2014	300	1.9

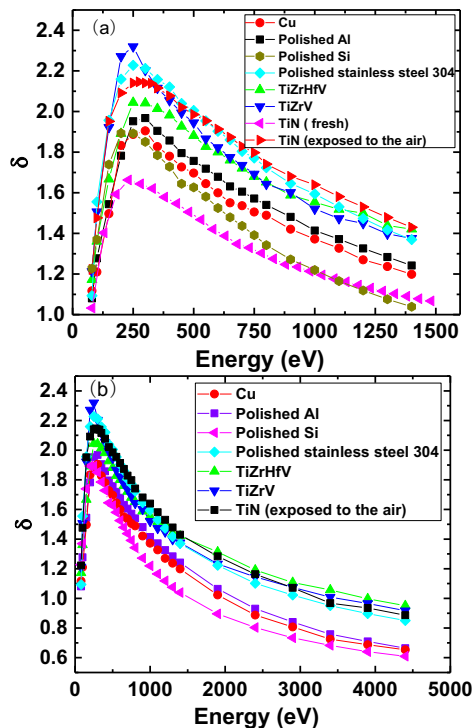
# Experimental measurement and theoretical research: SEY

## ➤ Conductive sample

$I_p=300\text{ nA}$

**Conclusion:** TiN (fresh) <polished Si<Cu<polished Al< TiZrHfV(nonactivated) < TiN (exposed) <Polished stainless steel 304< TiZrV(nonactivated).  $E_{pm}:250\text{ -}300\text{ eV}$

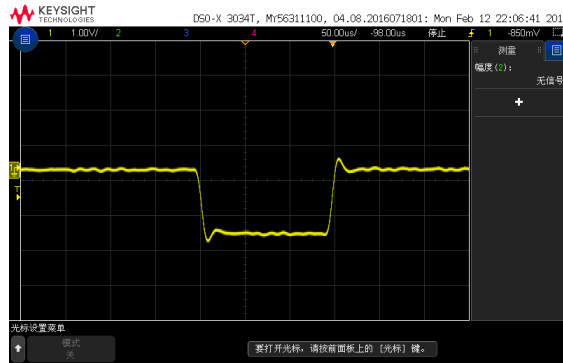
Due to the material of SEY is not only related to the material composition but also surface roughness , surface pollution and so on, the measurement results of the same material under different measuring condition and different devices will have differences.



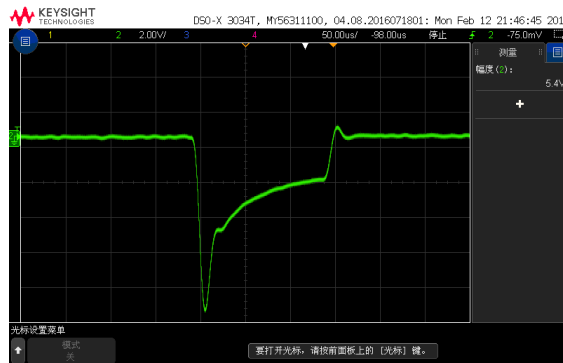
样品	$E_{pm}$ (eV)	$\delta_m$	$E_{pm}$ (eV) (reference)	$\delta_m$ (reference)
TiN (fresh)	230	1.66	300	1.5~2.4
Polished Si	200	1.89		
Cu	300	1.90	300	1.90
Polished Al	300	1.97	300	2.55
TiZrHfV	250	2.04		
TiN (expose for 3 month)	275	2.15	300	1.5~2.4
Polished stainless steel 304	250	2.23	300	2.25
TiZrV	250	2.32	250	1.3~2

# Experimental measurement and theoretical research: SEY

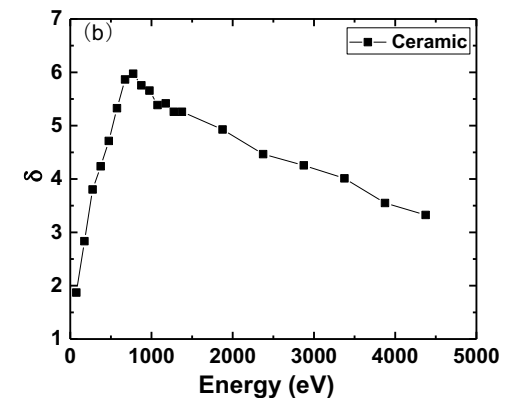
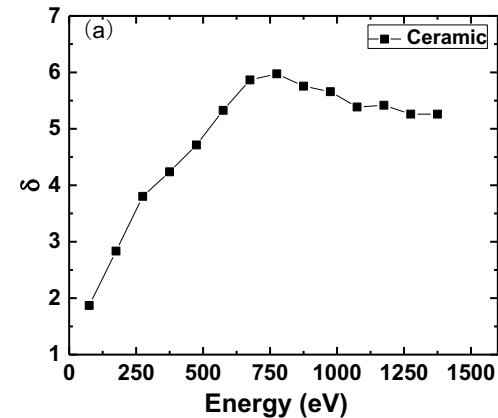
## ➤ Insulating sample



Voltage signal  $U_p$  at faraday cup measured by oscilloscope



Voltage signal  $U_s$  at the collector measured by oscilloscope after neutralization



SEY of ceramic samples

# Experimental measurement and theoretical research: SEY

## ➤ Insulating sample

**Conclusion:** The SEY of ceramic sample is very high, Primary energy 75 eV  $\rightarrow$  1.9,  $E_{pm}$ :775 eV  $\rightarrow$  5.97, constant with Dawson, P. H., 1966(6.4).

In order to reduce **the eddy current effect** on the vacuum chamber surface caused by the rapidly changing magnetic field in magnet in CSNS, ceramic is used as vacuum chamber material in the RCS ring, but the electron cloud effect caused by the high secondary electron yield will affect the stability of the proton beam, so the inner wall of the ceramic vacuum chamber was then plated with TiN films of suitable thickness with good vacuum properties and low secondary electron emission coefficient.

After coated with **TiN**, **5.97  $\rightarrow$  1.66**, rose to 2.15(exposed to the air for 3 month) due to contamination.

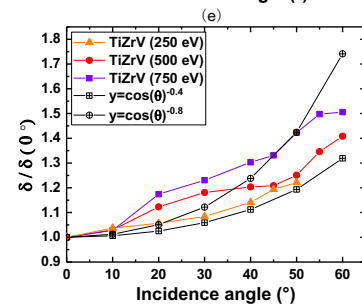
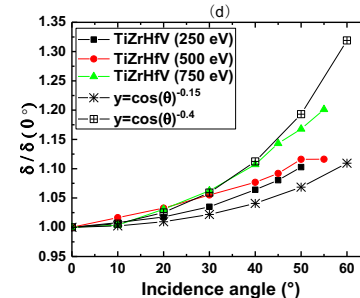
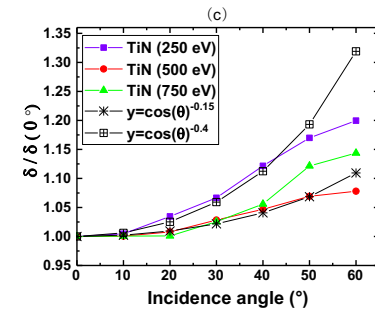
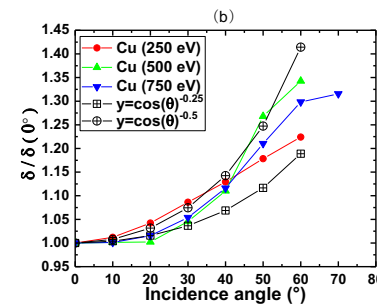
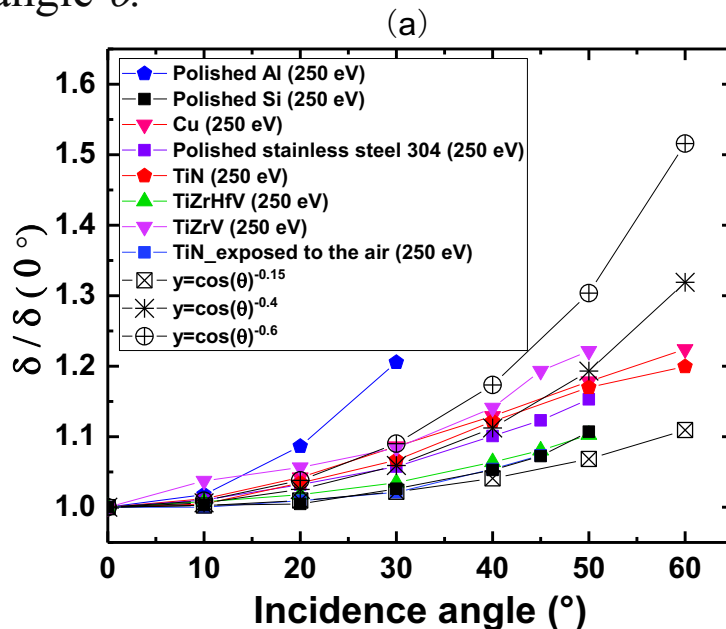
Sample	$E_{pm}$ (eV)	$\delta m$	$E_{pm}$ (reference)	$\delta m$ (reference)
ceramic	775	5.97	650	6.4
Coated with TiN (fresh)	230	1.66	300	1.5~2.4

# Experimental measurement and theoretical research: SEY's dependence on incidence angle

## ➤ Oblique incidence

Conclusion: In the range of  $0-60^\circ$ , the SEY gradually increases with the increase of the incident angle  $\theta$ , and has a **cosine** relationship with the incident angle. However, the SEY begins to decrease after the incident angle increased to  $60^\circ$ , which is consistent with the reference (Lin Zulun, 2013).

This may be because the **measurement error** increase with the increase of the incident angle  $\theta$ .



# Experimental measurement and theoretical research: SEY's dependence on incidence angle

Comparing the measurement results with the calculation results of the cosine function formula, it can be seen that the corresponding coefficients  $n$  of several materials range from about 0.16 to 0.80:

$$y = \cos(\theta)^{-n}$$

Where  $n$  is a parameter related to the material and the energy of the incident electrons.

Sample	$n$
Cu	0.25~0.50
TiN	0.15~0.40
TiZrHfV	0.15~0.40
TiZrV	0.40~0.80

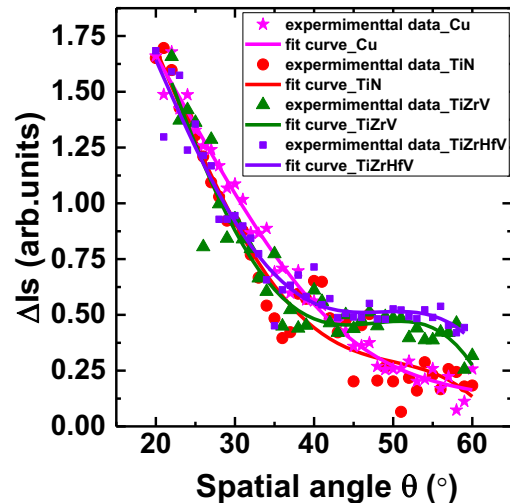
# Experimental measurement and theoretical research: Spatial distribution of secondary emission electrons

$E_p=600$  eV ,  $I_p=500$  nA

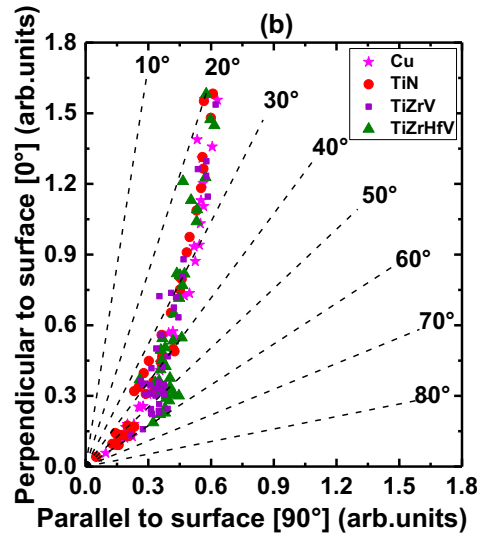
**Conclusion:** According to the theory (Ciappa et al., 2012), the number of true secondary electrons at the unit solid angle conforms to the following formula. The parameters obtained by fitting the measurement results using the formula are shown in the following table.

$$f(\theta) = \cos \theta (1 + a \sin^2 \theta + b \sin^4 \theta + \dots)$$

(a)



(b)



	a	b
Cu	-2.10	1.63
TiN	-1.24	1.91
TiZrHfV	-1.09	2.03
TiZrV	-0.96	1.99

Secondary Electron Spatial Distribution in Cartesian and Polar Coordinate Systems

Fitting parameters for different samples

# Experimental measurement and theoretical research: Spatial distribution of secondary emission electrons

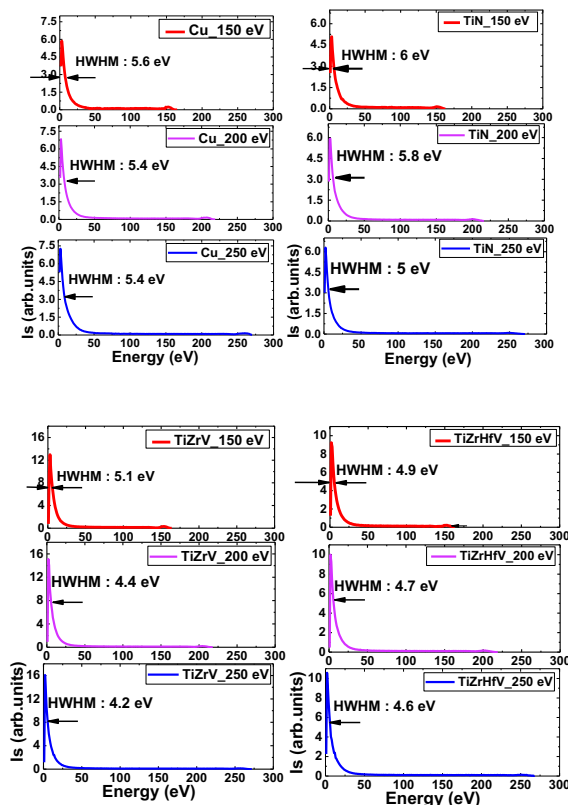
- **Measure the complete energy spectrum of secondary electrons and determine the proportion of different kinds of secondary electrons ;**
- **Calculated the full width at half maximum ( FWHM ) of the true secondary electron peak and the elastic reflected electron peak;**
- **Using the gaussian function to fit the secondary electron peak and the elastic reflected electron peak.**

# Experimental measurement and theoretical research: Spectrum distribution of secondary emission electrons

- Measure the complete energy spectrum of secondary electrons and determine the proportion of different kinds of secondary electrons

**Conclusion:**

0 ~ 50 eV(secondary electron peak ),  $E_p$ (elastic scattering peak),



Total secondary electron energy spectrum of different materials

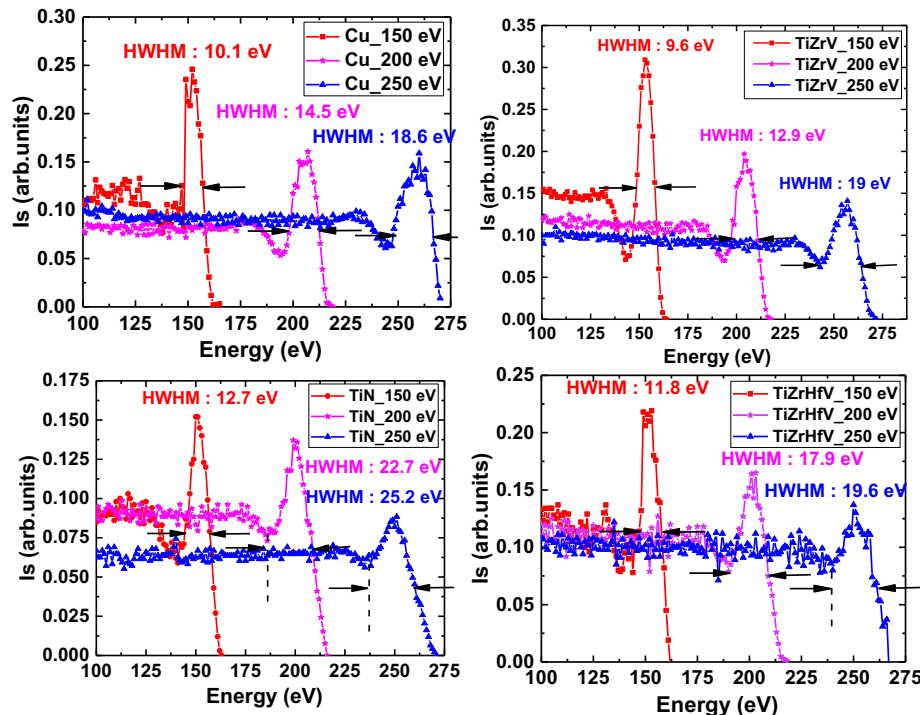
材料	$E_p$ (eV)	SE	ERE	IRE
Cu	150	80.2%	4.8%	15.0%
	200	79.9%	3.1%	17.0%
	250	76.8%	2.9%	20.3%
TiN	150	81.8%	3.3%	14.9%
	200	78.7%	3.5%	17.8%
	250	78.5%	3.0%	18.5%
TiZrHfV	150	83.5%	3.1%	13.4%
	200	80.7%	2.7%	16.6%
	250	78.5%	2.4%	19.1%
TiZrV	150	84.8%	2.8%	12.4%
	200	84.2%	2.2%	13.6%
	250	83.3%	1.8%	14.9%

The proportion of secondary electrons in each component  
(80%, 3%, 17%)

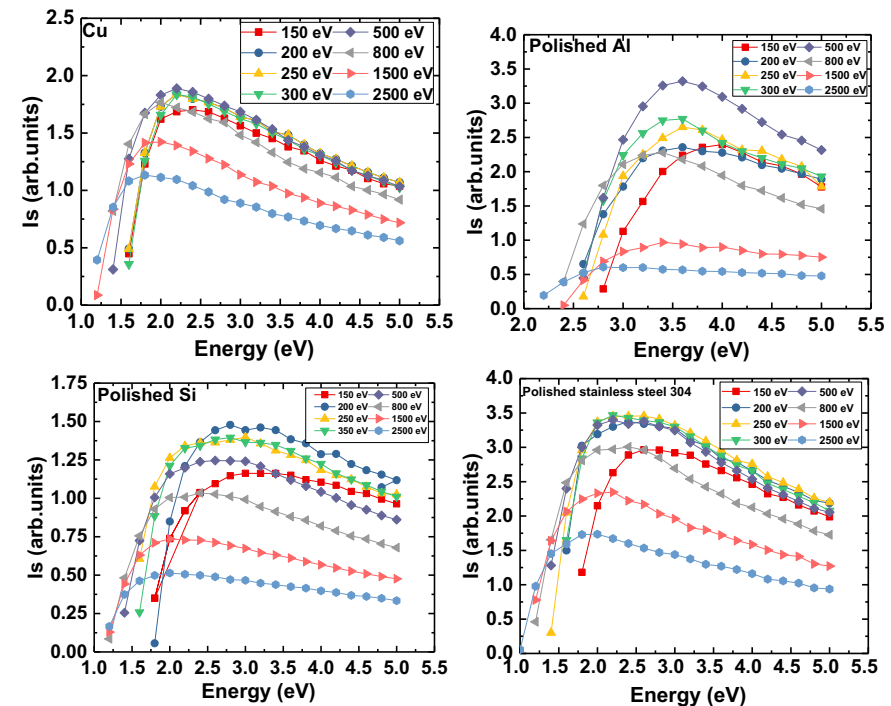
# Experimental measurement and theoretical research

The position of the true secondary electron peak changes very little with the change of the energy of the incident electron, but the position of the elastic scattering peak increases with the increase of the energy of the incident electron.

Generation mechanism: extranuclear electron, primary electron



Elastic scattering electron energy spectrum of different materials



True secondary electron energy spectrum of different materials

# Experimental measurement and theoretical research

- Calculated the full width at half maximum ( FWHM ) of the true secondary electron peak and the elastic reflected electron peak;

Conclusion: the position of energy spectrum peak is consistent with reference, and the half height and width is slightly larger than that of reference (Staib, Ph, and U. Dinklage, 1977)

Ep (eV)	Cu	Al	Si	Stainless steel 304	TiN	TiZrV
150	2.4	4.0	3.0	2.6	2.8	2.4
200	2.2	3.6	3.2	2.4	2.6	2.2
250	2.2	3.6	3.0	2.4	2.6	2.2
300	2.2	3.6	2.8	2.2	2.6	2.2
500	2.2	3.6	2.6	2.2	2.4	2
800	2.0	3.4	2.6	2.4	2.4	1.8
1500	2.0	3.4	2.0	2.2	2.0	1.6
2500	1.8	3.2	2.0	2.0	1.8	1.8

The position of the true secondary electron energy spectrum peak (eV) (2~4eV)

样品	Ep (eV)	SE (eV)	ERE (eV)
Cu	150	5.6	10.1
	200	5.4	14.5
	250	5.4	18.6
TiN	150	6.0	12.7
	200	5.8	22.7
	250	5.0	25.2
TiZrHfV	150	4.9	11.8
	200	4.7	17.9
	250	4.6	19.6
TiZrV	150	5.1	9.6
	200	4.4	12.9
	250	4.2	19.0

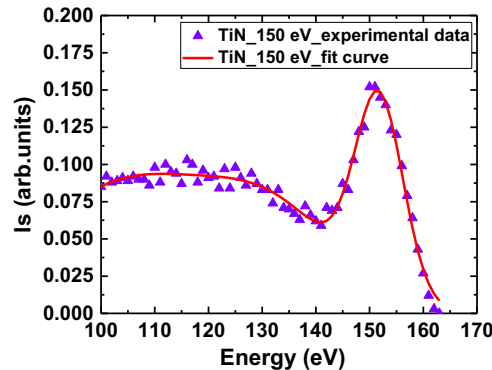
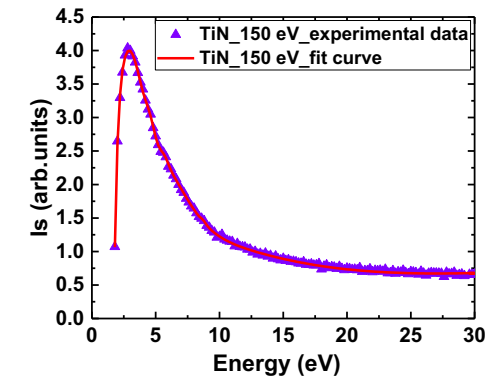
True secondary electron and elastic scattering electron energy spectrum half high and wide (5 eV, 16 eV)

# Experimental measurement and theoretical research

- Using the gaussian function to fit the secondary electron peak and the elastic reflected electron peak

Satisfy: gaussian distribution; For: simulation of electron clouds

$$f(x) = a_1 \times e^{-\frac{(x-b_1)^2}{c_1}} + a_2 \times e^{-\frac{(x-b_2)^2}{c_2}} + a_3 \times e^{-\frac{(x-b_3)^2}{c_3}} + \dots$$



TiN	a	b	c
1	-8.571e+004	-2.866	1.435
2	0.1676	4.559	0.5111
3	0.07829	5.701	0.3892
4	0.8744	4.833	3.082
5	1.425	122.1	103.8
6	0.02801	8.723	0.2728
7	1.664	2.793	1.48
8	2.352	-11.7	20.05
Goodness of fit (SE)			
SSE	0.001698		
R-square	0.9676		
Adjusted R-square	0.9629		
RMSE	0.005557		

TiN	a	b	c
1	0.1309	151.8	6.322
2	0.08781	105.3	25.11
3	0.05302	132.9	17.1
Goodness of fit (ERE)			
SSE	0.0546		
R-square	0.9995		
Adjusted R-square	0.9994		
RMSE	0.02151		

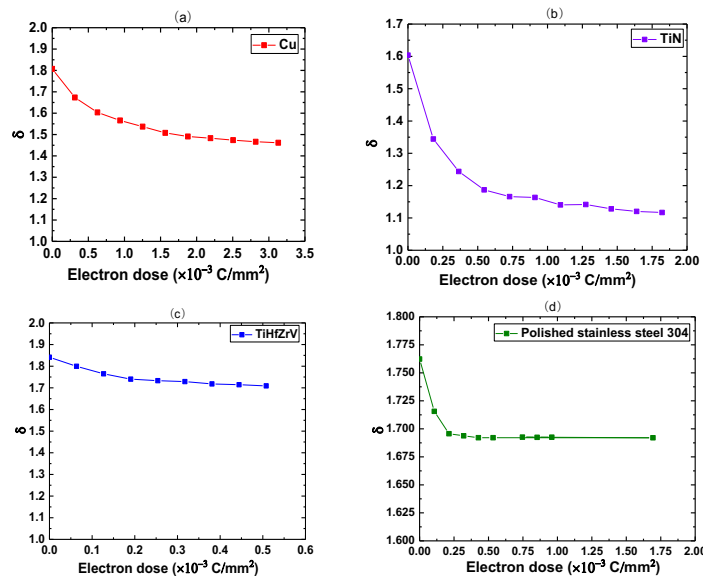
# Experimental measurement and theoretical research

$E_p=250 \text{ eV}$  ,  $I_p=0.6 \mu \text{ A}$

**Conclusion:** the SEY of each material decreases with the increase of incident electron dose and finally becomes stable.

**Analysis :** Electron bombardment can cause changes in the surface of the material, removing contaminants and oxides on the surface of the material, and even forming a carbon film on the surface, making the measured SEY lower (Larciprete R, 2013).

Bombardment reducing SEY is an effective secondary electron suppression measure.



Sample	$\delta_0$	$\delta$	Dose ( $\times 10^{-3} \text{ C/mm}^2$ )
Cu	1.81	1.46	3.13
TiN	1.60	1.12	1.82
TiHfZrV	1.84	1.71	0.51
Stainless steel 304	1.76	1.69	0.96

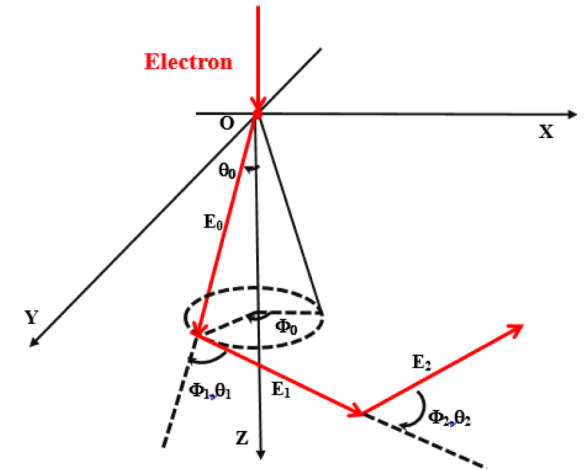
# Formula calculation and software simulation

## ➤ Formula

$$\delta_{e\theta} = \frac{K}{\varepsilon} \int_0^{\frac{1}{\alpha \cos \theta}} \frac{G}{E_{p0}} e^{-\alpha s \cos \theta} ds = \frac{KG(e-1)}{\varepsilon e E_{p0} \alpha \cos \theta} \quad (1)$$

$$\delta = 0.5 \times \frac{E_{p0}}{\varepsilon} \times \frac{\lambda}{R} (1 - e^{-R/\lambda}) \quad (2)$$

$$\frac{\delta}{\delta_m} = 1.28 \left( \frac{E_p}{E_p^m} \right)^{-0.67} (1 - \exp(-1.614 \left( \frac{E_p}{E_p^m} \right)^{1.67})) \quad (3)$$



## ➤ Casino

Based on Monte Carlo simulation method: A computer experimental method for simulating the motion of real particles using the idea of probability statistics.

(DEMERSH, 2011)

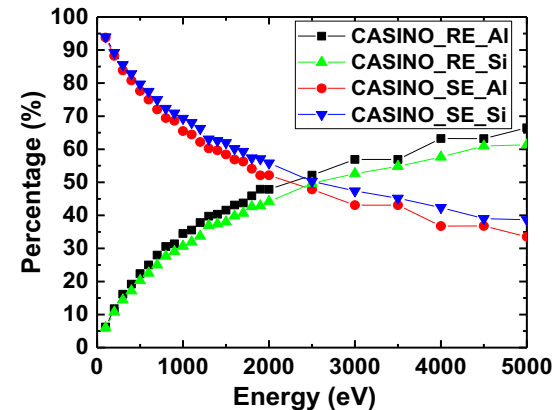
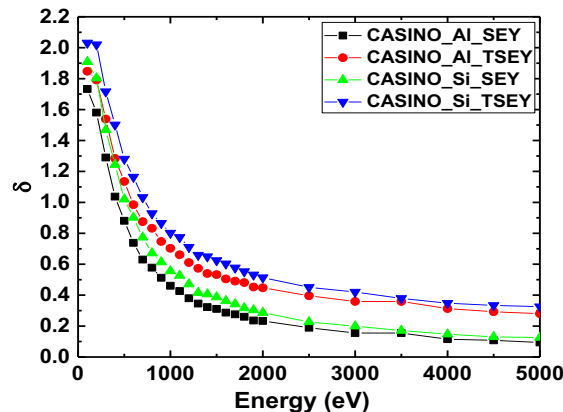
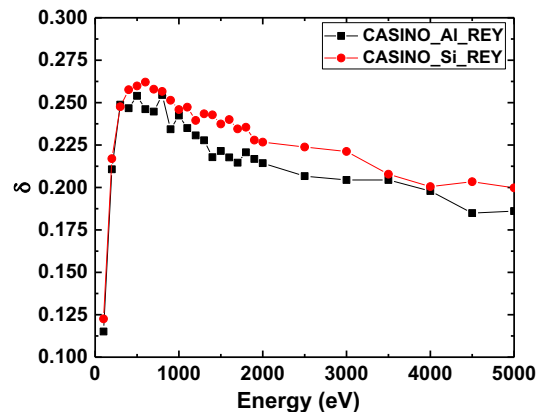
# Formula calculation and software simulation: SEY

## ➤ CASINO

### Conclusion:

As the energy of the incident electrons increases, the yield of backscattered electrons first increases and then decreases, and the yield of **true secondary electrons(SE)** and the **total secondary electrons(TSE)** continue to decrease. As the incident electron energy increases, the proportion of true secondary electrons (SE) decreases, and the proportion of **reflected electrons (RE)** increases.

The work function used in the simulation is the default value of the software, Al is 4.28 eV and Si is 4.85 eV

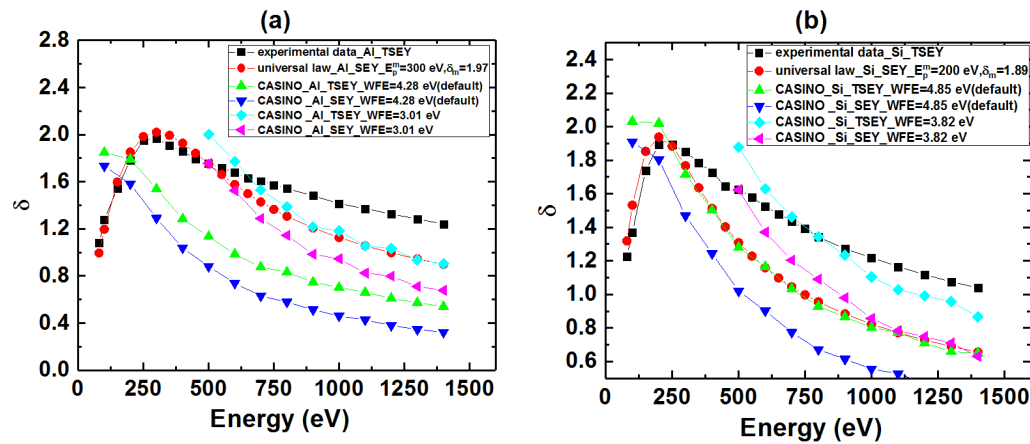


# Formula calculation and software simulation:SEY

The calculation result of formula (3) is consistent with the trend of experimental measurement results. Software simulation is consistent with experimental data after 500 eV. The numerical differences are as follows:

$$\frac{\delta}{\delta_m} = 1.28 \left( \frac{E_p}{E_p^m} \right)^{-0.67} (1 - \exp(-1.614 \left( \frac{E_p}{E_p^m} \right)^{1.67})) \quad (3)$$

- ①The theoretical formula is a result of a series of formulae **approximate derivation**, so there is a certain gap between the true value.
- ②The theoretical formula and software simulation only consider the nature of the **sample material itself**, and do not consider the state of **surface contamination, adsorption, roughness**, etc. Therefore, there is a certain gap between the actual value and the actual value.
- ③In the theoretical formulas and software simulations, **true secondary electron yields** are calculated, however the experiment measures the total secondary electron yield. The value of the total secondary electron yield is the sum of the true secondary electron yield value and the value of the backscattered electron yield. From the measurement analysis, it can be seen that the proportion of backscattered electrons increases with increasing incident energy. Therefore, the experimental measurement is slightly larger than the calculated value of the formula and the difference between the two increases gradually with the increase of energy.



# Summary and Prospect

## Summary

- The **differential method** was used to verify the measurement scheme of the secondary electron **spatial distribution**, and a multi-functional, high-efficiency secondary electron emission characteristic measurement platform capable of **simultaneously measuring secondary electron yield, energy spectrum distribution, and spatial distribution** was constructed.
- TiN (fresh) <polished Si<Cu<polished Al< TiZrHfV(**nonactivated**) < TiN (exposed) <Polished stainless steel 304< TiZrV(**nonactivated**)<ceramic. Epm:250 -300 eV,  $\delta m$ :1.66~2.32, **ceramic** after coated with TiN, 5.97  $\rightarrow$  1.66
- $\delta$  has **a cosine relationship** with the incident angle in  $0\sim 60^\circ$ .
- The spatial distribution satisfies **cosine distribution**.
- The spectrum distribution satisfies **gaussian distribution**
- SEY of each material **decreases** with the increase of incident electron dose and finally come to be **stable**

# Summary and Prospect

## Prospect

- **Further study on the new materials such as graphene**
- **Add heating and baking equipment**
- **Add low temperature superconducting equipment**
- **Upgrade to on-line measuring device**

**Thank you for your attention  
and advice!**